



## TECHNICAL PAPER

# Assessing the influence of fibers on the flexural behavior of reinforced concrete beams with different longitudinal reinforcement ratios

Antonio Conforti<sup>1</sup> | Raúl Zerbino<sup>2</sup> | Giovanni Plizzari<sup>1</sup>

<sup>1</sup>Department of Civil, Environmental, Architectural Engineering and Mathematics (DICATAM), University of Brescia, Italy

<sup>2</sup>Department of Civil Engineering, La Plata National University, La Plata, Argentina

**Correspondence**

Antonio Conforti, Assistant Professor, Department of Civil, Environmental, Architectural Engineering and Mathematics (DICATAM), University of Brescia, Italy.  
Email: antonio.conforti@unibs.it

**Abstract**

The use of fibers in reinforced concrete (RC) beams mainly improves both the bearing capacity and the cracking control. In this way, positive effects on the service life of RC structures can be expected. In this paper, the fiber influence on the flexural behavior of RC beams with different longitudinal reinforcement ratios ( $0.5\% \leq \rho_s \leq 1.2\%$ ) is analyzed by testing small-scale RC beams. Concretes incorporating 0, 25 and 50 kg/m<sup>3</sup> of steel, 6 and 12 kg/m<sup>3</sup> of glass macrofibers, and 5 and 10 kg/m<sup>3</sup> of polymer macrofibers were studied. Crack and deflection control, as well as bearing capacity and crack localization were evaluated for a broad range of fiber-reinforced concrete (FRC) toughness. It is verified that fibers, in the longitudinal reinforcement ratio considered, improve the bending behavior at serviceability limit state (SLS) and ultimate limit state (ULS) of RC beams, without limiting the structure ductility. It was also confirmed the philosophy of the *fib* Model Code 2010, such that FRC can be considered as a composite material where performance parameters govern its mechanical behavior. Finally, the several data available allowed to deeply analyze *fib* Model Code 2010 formulations (mean crack spacing and flexural bearing capacity) and to propose modifications where needed.

**KEYWORDS**

crack spacing, cracking control, fiber-reinforced concrete, flexure, longitudinal reinforcement ratio

## 1 | INTRODUCTION

The use of fiber-reinforced concrete (FRC) in beams with longitudinal conventional reinforcement (RC) improve deflection control,<sup>1–3</sup> crack control<sup>4–9</sup> shear resistance,<sup>10–13</sup> and in some cases flexural bearing capacity.<sup>3</sup> To the

contrary, FRC can provoke a crack localization (one flexural crack wider more than the other cracks do) after RC beam yielding that could reduce the element ductility.<sup>14–16</sup> Fibers transfer stresses across a crack leading to a more diffused crack pattern characterized by narrower and more closely spaced cracks,<sup>5,17</sup> while in shear they also enhance the aggregate interlock mechanism. Thanks to this improved crack control, positive effects on the service life of RC structures are expected. Apart shear, the fiber influence is related to the weighted ratio between FRC postcracking performances and longitudinal reinforcement ratio ( $\rho_s = A_s/(b_w d)$ ). The latter generally varies

Discussion on this paper must be submitted within two months of the print publication. The discussion will then be published in print, along with the authors' closure, if any, approximately nine months after the print publication.

between 0.6 and 1.2% for RC beam ductility reasons, while a very broad range of FRC toughness is now available in the market. However, the majority of studies present in the literature about the flexural behavior of RC beams deals with postcracking mechanical performances typical of steel fibers,<sup>1,3,7,9</sup> since very few studies consider other fiber types.<sup>14,18</sup> This underlines the need of studying FRC with different postcracking response as compared to steel fibers, in order to prove their effectiveness and evaluate code formulation accuracy.

The *fib* Model Code 2010<sup>19</sup> introduced FRC as structural material, providing design rules to take into account fiber effects properly; this represented a great contribution for further applications of fibers combined with conventional bars. Although most studies from which the Code formulations were developed were mainly related to steel fibers, this Code assume FRC as a composite material where performance parameters govern its mechanical behavior. In this way, as the effect of fibers is related to FRC toughness, regardless of fiber type and amount, different fibers can be considered (steel, polymer, glass, or others).

A recent paper presents the results of the first part of this research where different contents of steel, glass, or polymer macrofibres were incorporated in RC beams with a typical value of longitudinal reinforcement ratio equal to 0.9%.<sup>14</sup> In addition to the analysis of crack pattern and bearing capacity, the results were compared with the predictions of *fib* Model Code 2010.<sup>19</sup> This study concluded that for the used testing conditions the effect of fibers on the flexural behavior of RC beams is mainly related to FRC toughness (measured from the residual parameters  $f_{R1}$  and  $f_{R3}$ ), regardless of fiber type and amount. A significant reduction in crack spacing was mainly observed for high values of  $f_{R1}$ , while the fiber contribution on the reduction of the postcracking deflection resulted noteworthy for  $f_{R1} \geq 3$  MPa. For the used longitudinal reinforcement ratio and for the wide range of FRC toughness considered no reduction of RC beam ductility were seen, even if a crack localization occurred after rebar yielding in the majority of FRC samples. When considering the *fib* Model Code 2010 approach, the mean crack spacing predictions seemed to be characterized by a progressive increasing underestimation for FRC toughness increase.

Based on these encouragement conclusions and considering that further tests varying other principle variables should be necessary in order to improve the current *fib* Model Code 2010 prediction models, a second part of the research was performed. The influence of steel, glass, or polymer macrofibres on the crack pattern, the bearing capacity and the failure type of RC beams with longitudinal reinforcement ratios between 0.5% (value close to the lower bound adopted in practice) and 1.2% (upper bound

generally adopted in practice) is discussed in this paper. The experimental results are compared with the mean crack spacing and the strength capacity predictions of *fib* Model Code 2010. The flexural bearing capacity formulation resulted reliable, while some modification are proposed for the mean crack spacing one, since it was observed that the model adopted by *fib* Model Code 2010 to describe the postcracking strength in tension at serviceability limit state (SLS,  $f_{Fts}$ ) seems not to be representative for mean crack spacing estimations.

## 2 | RESEARCH SIGNIFICANCE

The present experimental program aims of clarifying the influence of a broad range of FRC toughness (considering steel, polymer and glass fibers in different amounts) on the flexural behavior (especially cracking control, deflection control, and possible limitation of ductility due to crack localization) of RC beams characterized by values of longitudinal reinforcement ratio typically adopted in practice and of evaluating *fib* Model Code 2010 formulations. The influence of fibers different than steel ones is still not well-studied and it was not directly considered in the development of most *fib* Model Code 2010 equations. Results underlines that the effects of fibers is mainly related to their postcracking strengths (with linear relations between main parameters) and that the ductility reduction is not an issue. In addition, *fib* Model Code 2010 formulation for mean crack spacing prediction was improved by proposing to use a residual tensile strength at crack opening equal to 0.15 mm ( $\sigma_{0.15}$ ) instead of  $f_{Fts}$ . This will allow designers to estimate with higher accuracy both mean crack spacing and crack width of FRC elements.

## 3 | EXPERIMENTAL PROGRAM

The study was performed on seven types of concrete mixtures, a reference plain concrete (CONTROL) and six FRC, two incorporating 25 or 50 kg/m<sup>3</sup> of hooked-end steel fibers 50 mm long and 1 mm diameter (S-25 and S-50), two adding 6 or 12 kg/m<sup>3</sup> of 36mm long and 0.54mm diameter crimped glass macrofibers (G-6 and G-12) and two with 5 or 10 kg/m<sup>3</sup> of 58mm long and 0.67mm diameter embossed polymer macrofibers (P-5 and P-10). Fiber type and amount were chosen in order to obtain a broad range of FRC toughness and to be coherent with the first part of this research.<sup>14</sup> More details on fibers properties and postcracking performances can be found in Conforti et al.<sup>14</sup>

All concretes were prepared from the same base concrete using Portland cement, natural siliceous sand,

12mm maximum size granitic crushed stone, and 0.41 water/cement ratio. A high-range polycarboxylate-based superplasticizer was added in each concrete in order to obtain a slump of  $60 \pm 10$  mm.

Three RC beams (more details in Section 3.1), three standard beams (according to EN 14651<sup>20</sup>), and six  $100 \times 200$  mm cylinders were produced for each concrete (for a total of 42 RC beams). All specimens were cured in moist room for 28 days and then remain in laboratory indoor up to testing. Testing ages were between 60 and 90 days in order to minimize the variation of concrete mechanical properties during the testing period (both standard beams and cylinders were tested at the same age of RC beams).

Table 1 presents the mechanical properties of each concrete: the mean values of the compressive strength ( $f_c$ ) from cylinders, and the nominal stress at limit of proportionality ( $f_L$ ) and the residual strengths at crack mouth opening displacement (CMOD) of 0.5, 1.5, 2.5, and 3.5 mm ( $f_{R,1}$ ,  $f_{R,2}$ ,  $f_{R,3}$  and  $f_{R,4}$ ) from standard beams.<sup>20</sup> It can be observed that the compressive strength (48 MPa on average) and the postcracking residual strengths ( $1.8 \leq f_{R,1} \leq 5.4$  MPa and  $1.0 \leq f_{R,3} \leq 4.9$  MPa) of different concretes are similar to the one adopted by Conforti et al.<sup>14</sup> Therefore, the postcracking response of the different FRC in terms of nominal stress versus CMOD curves is analogous to the one previously showed. This allows in the following to directly compare the results of this research to those obtained in the former experience.

### 3.1 | RC specimen geometry, reinforcement and testing details

As first step, RC beams 150 mm high ( $h$ ) with a typical value of longitudinal reinforcement ratio  $\rho_s$  (0.9%, 2 bars

of 10 mm diameter) were tested.<sup>14</sup> With the aim of analyzing the fiber effect varying the longitudinal reinforcement ratio (and thus the diameter-to-effective reinforcement ratio  $\emptyset/\rho_{s,ef}$ , which is a key parameter in the cracking behavior of RC beams), the study was repeated on RC beams 150 mm high with  $\rho_s$  of 0.5 and 1.2% (bars of 8 and of 12 mm diameter, respectively). The clear concrete cover ( $c$ ) was kept constant and equal to 25 mm.

Figure 1 shows the geometry and reinforcement details of the RC specimens. Some pictures of steel cages and molds before casting are shown in Figure 1 as well. According to *fib* Model Code 2010 formulations for defining the effective area of concrete in tension ( $A_{c,ef}$ ), series 0.5 and 1.2% are characterized by  $\emptyset/\rho_{s,ef}$  (where  $\rho_{s,ef} = A_s/A_{c,ef}$ ) equal to 478 and 279 mm, respectively. The series 0.9% previously tested has instead a  $\rho_{s,ef} = 379$  mm. Stirrups were introduced near the supports to prevent a shear failure; the first stirrup was placed at half times the effective depth from point loads to avoid influence on sample crack pattern in the middle-third of the RC beam. It should be noted that the adopted sample geometry is expected to have a similar fiber orientation of standard beams,<sup>20</sup> since cross section and mold geometry are identical; this allows to better relate the sample response to the material toughness.

Rebar properties were characterized according to EN15630-1<sup>21</sup> by testing 600mm long pieces. The overall mean values of  $f_y$  and  $f_u$  resulted equal to:

- 469.4 MPa (CV = 0.01) and 632.3 MPa (CV = 0.02) for  $\emptyset 6$  stirrups;
- 602.8 MPa (CV = 0.01) and 685.2 MPa (CV = 0.01) for  $\emptyset 8$  reinforcing bars;

**TABLE 1** Compressive and bending (EN14651) properties of concretes (CV in brackets)

Series	$f_c$ (MPa)	$f_L$ (MPa)	$f_{R,1}$ (MPa)	$f_{R,2}$ (MPa)	$f_{R,3}$ (MPa)	$f_{R,4}$ (MPa)
CONTROL	46.2 (0.04)	4.54 (0.07)	—	—	—	—
S-25	45.2 (0.02)	5.13 (0.03)	3.86 (0.21)	3.89 (0.26)	3.52 (0.27)	3.33 (0.29)
S-50	46.8 (0.01)	5.10 (0.08)	5.43 (0.16)	5.29 (0.08)	4.94 (0.06)	4.58 (0.05)
G-6	48.6 (0.01)	4.84 (0.03)	1.99 (0.19)	1.60 (0.17)	1.05 (0.16)	0.68 (0.20)
G-12	48.9 (0.02)	4.92 (0.05)	3.12 (0.14)	2.71 (0.15)	1.73 (0.12)	1.13 (0.10)
P-5	54.6 (0.02)	5.10 (0.07)	1.79 (0.07)	1.89 (0.13)	2.14 (0.09)	2.25 (0.08)
P-10	45.8 (0.04)	4.59 (0.04)	2.58 (0.07)	3.11 (0.17)	3.57 (0.16)	3.74 (0.17)

- 505.1 MPa (CV = 0.02) and 612.3 MPa (CV = 0.01) for  $\text{Ø}12$  reinforcing bars.

RC beams were tested in displacement control using an INSTRON machine with a loading capacity of 1,000 kN using four-point loading configuration over net span of 840 mm (Figure 1). A LVDT was placed on a frame fixed at the neutral axis over each support for the measurement of the net mid-span deflection ( $\delta$ ) and a second LVDT was placed at the bottom face level of the RC beam with the aim of evaluating the extensibility and the sum of crack openings in the middle third of the RC beam during the test. Crack width and crack patterns were captured at different load stages: load corresponding to a stress on rebars of 340 MPa, load corresponding to a stress on rebars of 480 MPa, load of rebar yielding in RC beam without fibers, deflection of 5, 8, 12, and 16 mm. Specimens were monotonically loaded with a rate of 0.3 mm/min; at each load stage, the displacement was held while the cracks were evaluated using a comparator and a magnifying glass.

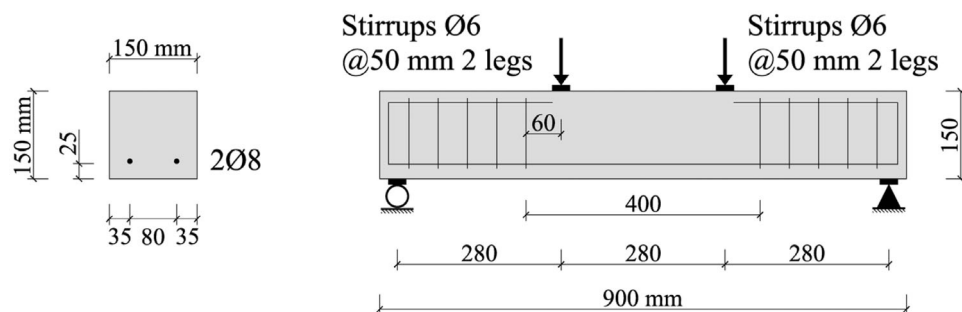
#### 4 | RESULTS AND DISCUSSION

All RC beams belong to series 0.5 and 1.2% showed a flexural failure characterized by steel yielding before the

concrete in the compression zone reaches its maximum useable strain (under reinforced beams). As shown in Figure 2, where the load versus net mid-span deflection mean curves of series 0.5% (Figure 2a) and 1.2% (Figure 2b) are reported, the failure was reached after the three typical stage: an initial uncracked stage (up to the flexural cracking load,  $P_{cr}$ ), a cracked stage (which includes crack formation and stabilized crack stage), and steel yielding stage. For both longitudinal reinforcement ratios, the fiber influence was not observed neither on  $P_{cr}$  nor on the onset of stabilized crack stage. A clear fiber influence, which magnitude varies as a function of rebar amount and FRC toughness, was instead observed on crack width, crack spacing, deflection, maximum load and crack localization. Table 2 and Table 3 summarize the mean values (coefficient of variation CV in brackets) of the main experimental results in terms of:

- Flexural cracking load ( $P_{cr}$ )
- Net mid-span deflection at steel stress of 340 MPa, which corresponds to a load of 26 kN ( $\delta_{P26}$ ) and 55 kN ( $\delta_{P55}$ ) for series 0.5 and 1.2%, respectively;
- Maximum flexural crack width at steel stress of 480 MPa, which corresponds to a load of 37 kN ( $w_{\max,P37}$ ) and 78 kN ( $w_{\max,P78}$ ) for series 0.5 and 1.2%, respectively;

##### Beams with $\rho_s = 0.5\%$



##### Beams with $\rho_s = 1.2\%$

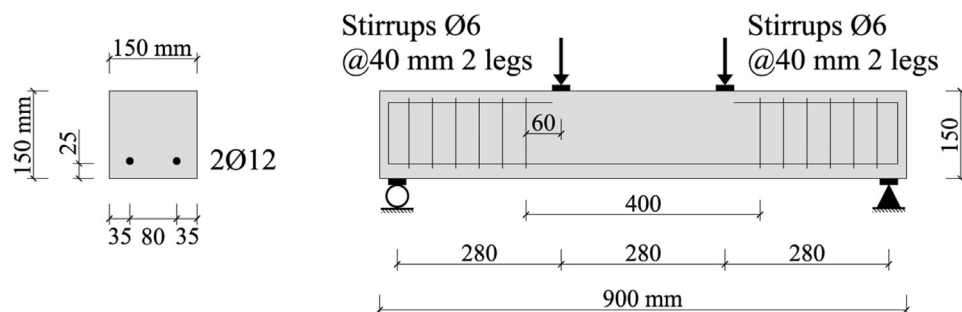
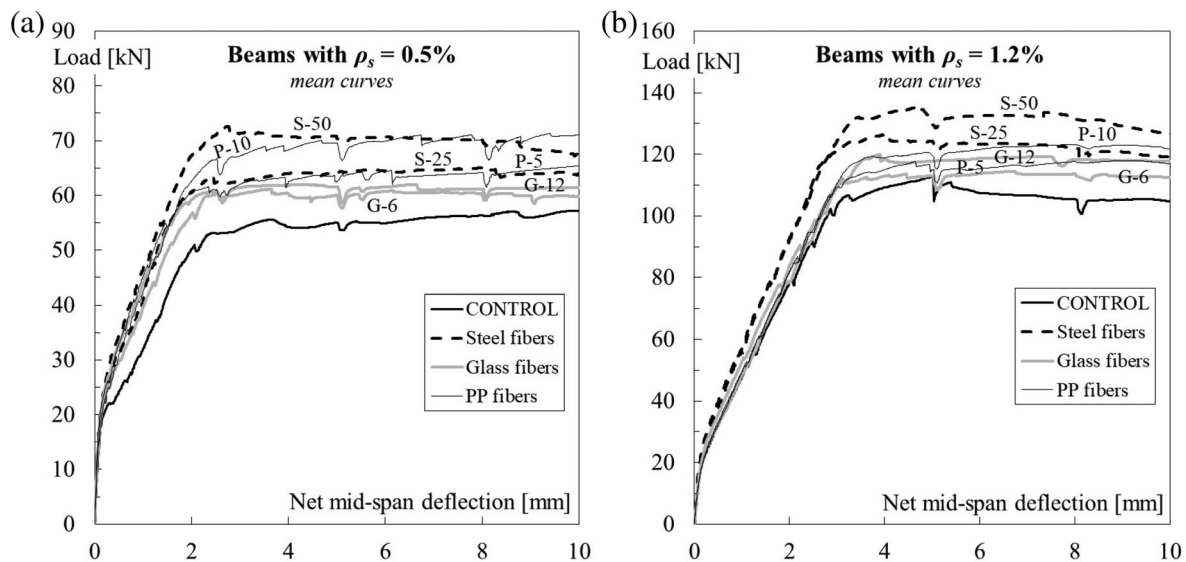


FIGURE 1 Geometry, reinforcement details and loading scheme of reinforced concrete beams with  $\rho_s = 0.5\%$  and  $\rho_s = 1.2\%$



**FIGURE 2** Load versus net mid-span deflection mean curves (up to 10 mm) of samples with longitudinal reinforcement ratios of 0.5% (a) and 1.2% (b)

**TABLE 2** Experimental results of flexural tests on reinforced concrete beams with  $\rho_s = 0.5\%$

	$P_{cr}$ (kN)	$\delta_{P26}$ (mm)	$w_{max,P37}$ (mm)	$s_r$ (mm)	$\delta_{CL}$ (mm)	$P_{max}$ (kN)	$\delta_u$ (mm)
CONTROL	16.9 (0.04)	0.61 (0.09)	0.20 (0.00)	118 (0.20)	— — —	58.2 (0.01)	20.6 (0.04)
S-25	16.7 (0.11)	0.33 (0.11)	0.15 (0.00)	85 (0.09)	2.0 2.5 —	65.5 (0.02)	21.2 (0.05)
S-50	16.5 (0.06)	0.24 (0.27)	0.10 (0.71)	76 (0.08)	2.8 3.0 3.1	74.6 (0.01)	19.8 (0.04)
G-6	15.9 (0.05)	0.38 (0.24)	0.18 (0.16)	104 (0.06)	— — 2.0	62.5 (0.03)	23.1 (0.10)
G-12	15.6 (0.03)	0.30 (0.11)	0.16 (0.09)	90 (0.11)	2.5 2.5 2.0	62.7 (0.01)	18.8 (0.11)
P-5	16.4 (0.03)	0.33 (0.04)	0.18 (0.20)	109 (0.02)	— — —	67.0 (0.01)	20.2 (0.02)
P-10	14.0 (0.16)	0.35 (0.17)	0.15 (0.00)	90 (0.15)	2.5 2.5 —	73.5 (0.04)	20.6 (0.02)

- Mean crack spacing at crack stabilized stage ( $s_r$ );
- Net mid-span deflection at crack localization initiation ( $\delta_{CL}$ );
- Maximum load ( $P_{max}$ );
- Maximum net mid-span deflection ( $\delta_u$ ).

Concerning the distance between stabilized cracks, Figure 3a and Figure 3b show the fiber influence on

mean crack spacing of RC beams as a function of  $f_{RI}$  (postcracking parameter of fib Model Code 2010 related to SLS) and  $\emptyset/\rho_{s,ef}$ . The latter is a key parameter for the evaluation of  $s_r$ , as proved by many building code formulations. It can be observed that, even varying the rebar amount, there is a quite strong linear correlation between  $s_r$  and  $f_{RI}$ , confirming the independence of this relation from fiber type. An increase of longitudinal

	$P_{cr}$ (kN)	$\delta_{P55}$ (mm)	$w_{max,P78}$ (mm)	$s_r$ (mm)	$\delta_{CL}$ (mm)	$P_{max}$ (kN)	$\delta_u$ (mm)
CONTROL	16.9 (0.15)	1.21 (0.02)	0.23 (0.12)	73 (0.06)	— — —	112.9 (—)	14.9 (0.22)
S-25	16.6 (0.06)	0.94 (0.03)	0.18 (0.16)	65 (0.09)	— — —	126.7 (0.06)	13.6 (0.26)
S-50	16.9 (0.18)	0.91 (0.09)	0.18 (0.20)	59 (0.01)	2.0 3.6 2.8	135.5 (0.02)	14.5 (0.24)
G-6	16.0 (0.05)	1.23 (0.04)	0.20 (0.00)	73 (0.10)	— — —	115.5 (0.02)	15.4 (0.20)
G-12	16.7 (0.04)	1.12 (0.01)	0.18 (0.20)	67 (0.07)	3.0 2.1 2.6	120.3 (0.01)	13.7 (0.21)
P-5	15.7 (0.06)	1.21 (0.18)	0.20 (0.00)	72 (0.04)	— — —	116.0 (0.07)	14.9 (0.27)
P-10	15.3 (0.12)	1.22 (0.16)	0.18 (0.20)	67 (0.10)	— — —	121.6 (0.02)	17.4 (—)

**TABLE 3** Experimental results of flexural tests on reinforced concrete beams with  $\rho_s = 1.2\%$

reinforcement ratio results in a decrease of the slope of the linear correlation, leading to have a fiber influence varying between 8 to 36% with  $\rho_s = 0.5\%$  and between 0 to 19% with  $\rho_s = 1.2\%$ . Consequently, for values of  $f_{RI}$  ranging between 1.5 and 3 MPa (P-5, P-10, G-6, and G12), the reduction of crack spacing due to fibers is remarkable only for  $\rho_s = 0.5\%$  and  $\rho_s = 0.9\%$ , while it is negligible for the upper bound of longitudinal reinforcement ratio. In fact, in the case of  $\rho_s = 1.2\%$ , only steel fibers are able to provide significant tension softening stresses across a crack that are able to reduce the crack spacing more than 10%. In Figure 3b, since several formulations model linearly the relation between  $s_r$  and  $\emptyset/\rho_{s,ef}$ , a linear regression was adopted. It can be underlined that a strong linear relation is present in CONTROL beams (the coefficient of determination  $R^2$  is very close to 1), confirming the good interpretation of the phenomenon by the actual formulations. Adding fibers, this relation continues to be linear regardless fiber type (with high values of  $R^2$ ), even if both slope and vertical axis-intercept vary. In other words, an increase of  $f_{RI}$  leads to a decrease of line slope. An increase of  $\emptyset/\rho_{s,ef}$  results in a higher crack spacing reduction due to fibers. It seems also that, projecting the different lines, no difference between CONTROL and FRC beams is expected for  $\emptyset/\rho_{s,ef} \approx 200$  (even if this values of  $\emptyset/\rho_{s,ef}$  are generally not adopted in practice since they corresponds to very high longitudinal reinforcement ratio).

The mean crack spacing formulation proposed by *fib* Model Code 2010<sup>19</sup> for RC and FRC elements was evaluating comparing its predictions ( $s_{r,MC2010}$ ) against the present results. Equation (1) can be derived from *fib* Model Code 2010<sup>19</sup> considering  $w_{max} = 1.7 w_m$ :

$$s_{r,MC2010} = 1.17 \cdot l_{s,max} = 1.17 \cdot \left[ k \cdot c + \frac{1}{4} \cdot \frac{\emptyset}{\rho_{s,ef}} \cdot \frac{(f_{ct} - f_{Fts})}{\tau_b} \right] \quad (1)$$

where  $l_{s,max}$  is the introduction length,  $k$  is an empirical parameter that can be assumed equal to 1,  $f_{ct}$  is concrete tensile strength (evaluating according to *fib* Model Code 2010), and  $\tau_b$  is the mean bond strength between rebars and concrete (considered as  $1.8f_{ct}$ ). The fiber influence is modeled by the SLS parameter ( $f_{Fts} = 0.45f_{RI}$ ) obtained from the linear simplified axial tensile stress-crack opening law (based on bending test results). Predictions were calculated by assuming strength reduction factors equal to 1 and the mean values of the material mechanical properties. Figure 3c reports the comparison between the experimental and predicted crack spacing ( $s_r/s_{r,MC2010}$ ) for the different longitudinal reinforcement ratio. It can be observed that, a small crack spacing is generally predicted by *fib* Model Code 2010<sup>19</sup> for both RC and FRC, even if good estimation are given up to values of  $f_{RI}$  of

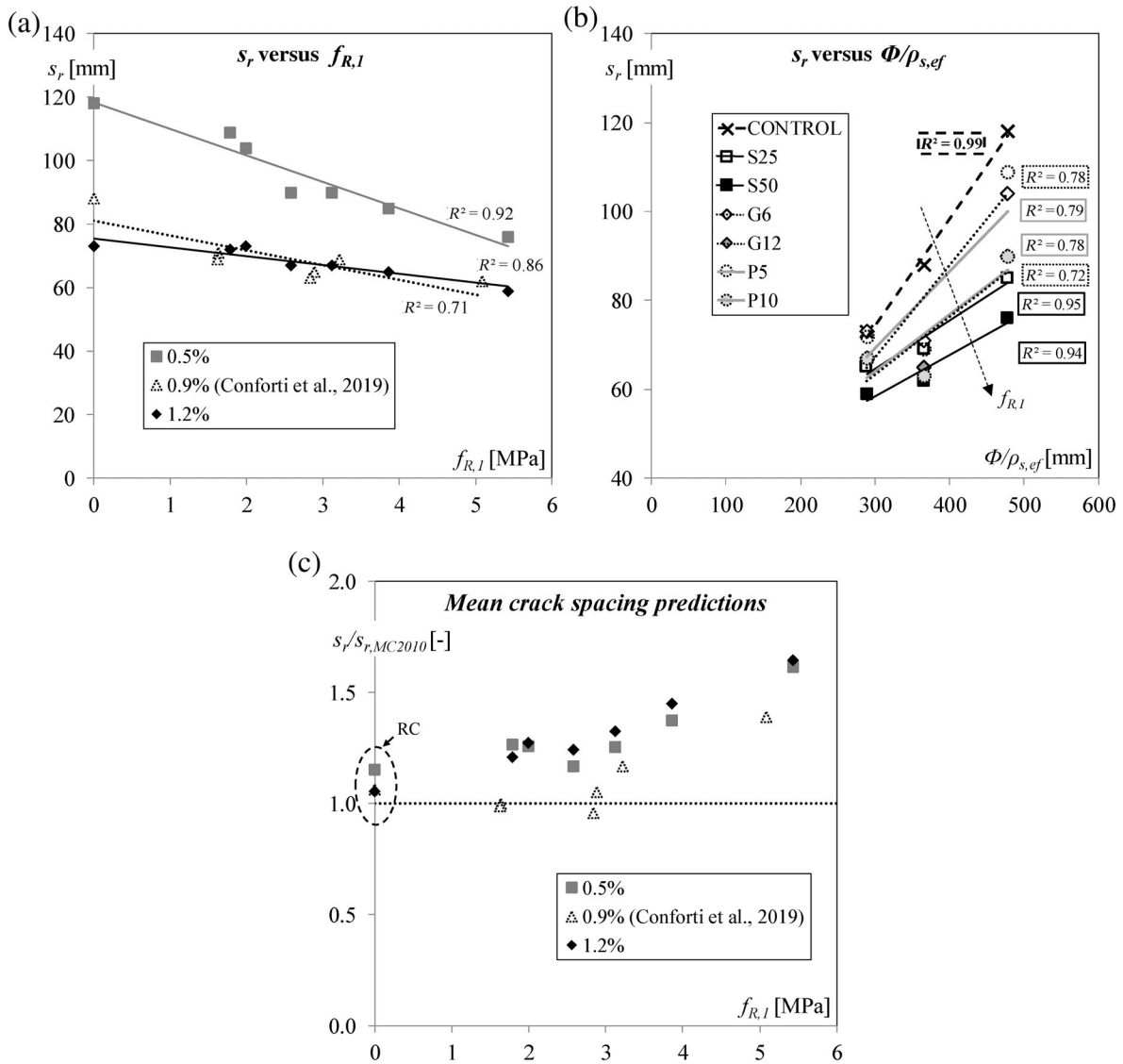


**FIGURE 3** Influence of fiber reinforced concrete on mean crack spacing of reinforced concrete beams as a function of  $f_{R,I}$  (a) and  $\Phi/\rho_{s,ef}$  (b); crack spacing predictions of *fib* Model Code 2010 (c)

about 3.5 MPa. In fact, after this value, for the three longitudinal reinforcement ratios studied, there is a similar progressive reduction of model accuracy. This proves that *fib* Model Code 2010 correctly model the  $\Phi/\rho_{s,ef}$  influence, while some improvement are required on the way of considering fiber effect.

Figure 4a shows the influence of the residual strength  $f_{R,I}$  on the maximum crack width. The latter was evaluated at a stress level on rebars of 480 MPa. It came out that a linear relation is possible in all cases. A clear maximum crack width reduction is visible for  $f_{R,I}$  greater than 2 MPa. In fact, for  $f_{R,I} < 2$  MPa (P-5 and G-6) the reduction is lower than 10%, while for higher values of  $f_{R,I}$  this reduction ranges between 10 to 50%, 40 and 22% for  $\rho_s$  equal to 0.5, 0.9, and 1.2%, respectively. The more effective fibers resulted the steel one in

both amounts (S-25 and S-50) and glass fibers in the highest amount (G-12), while polypropylene fibers P-10 leads to a reduction of about 10–20%. This evidence, as already underlined by Conforti et al.,<sup>14</sup> is due to the lower postcracking performances provided by polymer macrofibres for small crack opening as compared to other fiber types.

Another important parameter that could be influenced by the presence of fibers is the postcracking deflection.<sup>1</sup> As shown in Figure 2, the presence of fibers led to a deflection reduction at cracked stage different between RC beams of series  $\rho_s = 0.5\%$  (Figure 2a) and  $\rho_s = 1.2\%$  (Figure 2b). In order to quantify this difference, Figure 4b reports the postcracking deflection normalized to the one of CONTROL beams ( $\delta/\delta_{CONTROL}$ ) at steel stress of 340 MPa as a function of  $f_{R,I}$ . The latter was once

again chosen, since the deflection control is a typical verification at SLS. It came out that for  $\rho_s \geq 0.9\%$  the reduction of deflection due to fiber was significant only in the case of  $f_{R1} > 3\text{--}3.5$  MPa, which was the case of steel FRC (S-25 and S-50). To the contrary, for lower values of  $\rho_s$  (in this case 0.5%) all FRC (P-5 and G-6) provoke a deflection reduction varying between 38 to 60%. This is due to the significant tension softening transfer across flexural cracks by fibers as compared to the tension stiffening effect present in RC beams with low longitudinal reinforcement ratio. In addition, even if a linear regression again adopted for linking the deflection to  $f_{R1}$ , lower values of  $R^2$  were obtained in the case of  $\rho_s = 0.5\%$  and  $\rho_s = 1.2\%$ . Finally, it should be underlined that when RC

beams are made by using a very low amount of longitudinal reinforcement ratio ( $\rho_s \ll 0.5\%$ ), FRC creep could lead to a non-negligible increase of crack width and beam deflection.<sup>22</sup> Additional studies in this respect are needed, even if very low values of longitudinal reinforcement ratio are generally not adopted in practice.

Regarding the fiber influence on flexural bearing capacity, Figure 5a shows the ratio between  $P_{\max}$  and  $P_{\max}$  of the CONTROL beams as a function of the post-cracking parameter of *fib* Model Code 2010 related to ultimate limit state (ULS), that is,  $f_{R3}$ . It can be observed that, as expected, the increment of capacity is limited, especially in the case of  $\rho_s \geq 0.9\%$ . In the latter case the increment is up to 10%, while it reaches 25% with

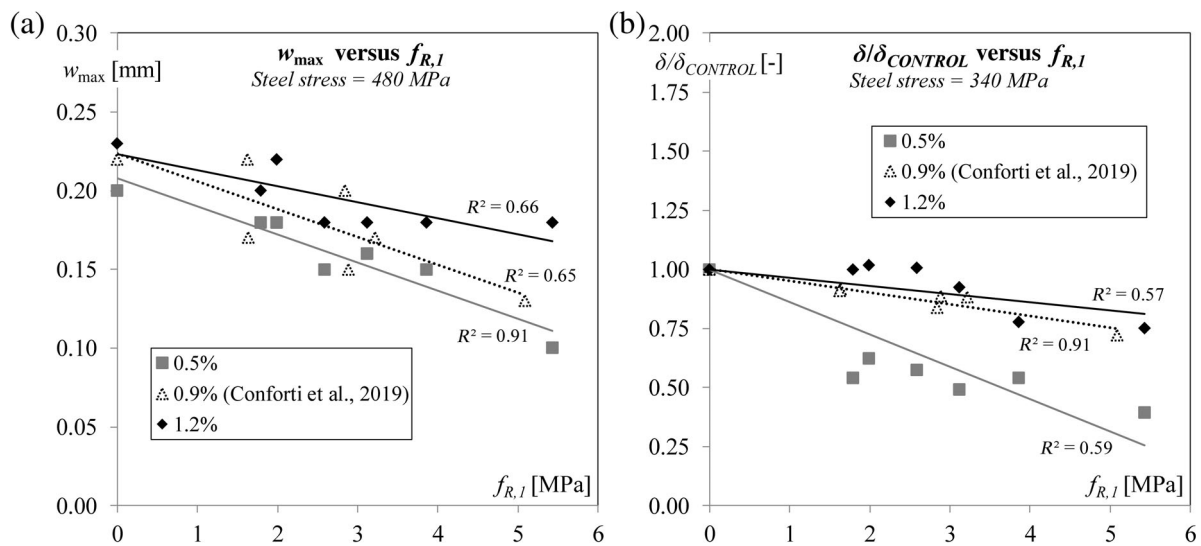


FIGURE 4 Influence of the residual strength  $f_{R,1}$  on the maximum crack width (a) and postcracking deflection (b)

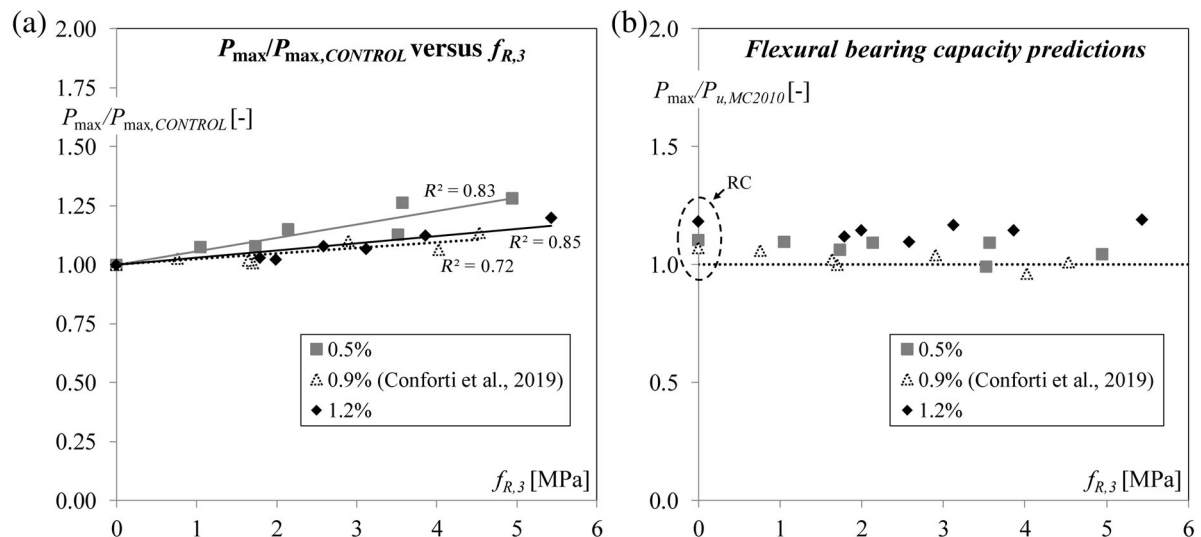


FIGURE 5 Influence of fiber reinforced concrete on the maximum bearing capacity of reinforced concrete beams (a) and flexural strength predictions of *fib* Model Code 2010 (b)

$\rho_s = 0.5\%$ . However, for all longitudinal reinforcement ratios studied, it came out that, only steel fibers concretes (S-25 and S-50) or high dosage polymer macrofibers concrete (P-10), due to their important postcracking performance at ULS ( $f_{R3} > 3$  MPa), are able to increase the flexural bearing capacity in a remarkable way. In the other cases, even if fibers influence is present, it can be neglected.

To consider fiber effect in flexural bearing capacity design, *fib* Model Code 2010 suggests to model fibers in sectional analyses as a constant stress under the neutral axis corresponding to the residual tensile strength

in uniaxial tension  $f_{Ftu} = f_{R3}/3$  (rigid plastic model). The predictions of this model are reported in Figure 5b, where the ratio between  $P_{max}$  and the load corresponding to the predicted flexural strength of *fib* Model Code 2010 ( $P_{max,MC2010}$ ) is shown as a function of  $f_{R3}$  for each longitudinal reinforcement ratio. It is worth mentioning that, for the typical values of longitudinal reinforcement ratios adopted in practice, *fib* Model Code 2010 predictions are reliable and consistent ( $P_{max}/P_{max,MC2010} = 1.06$  on average) also for RC beams with fibers. Therefore, modifications to this model are not required.

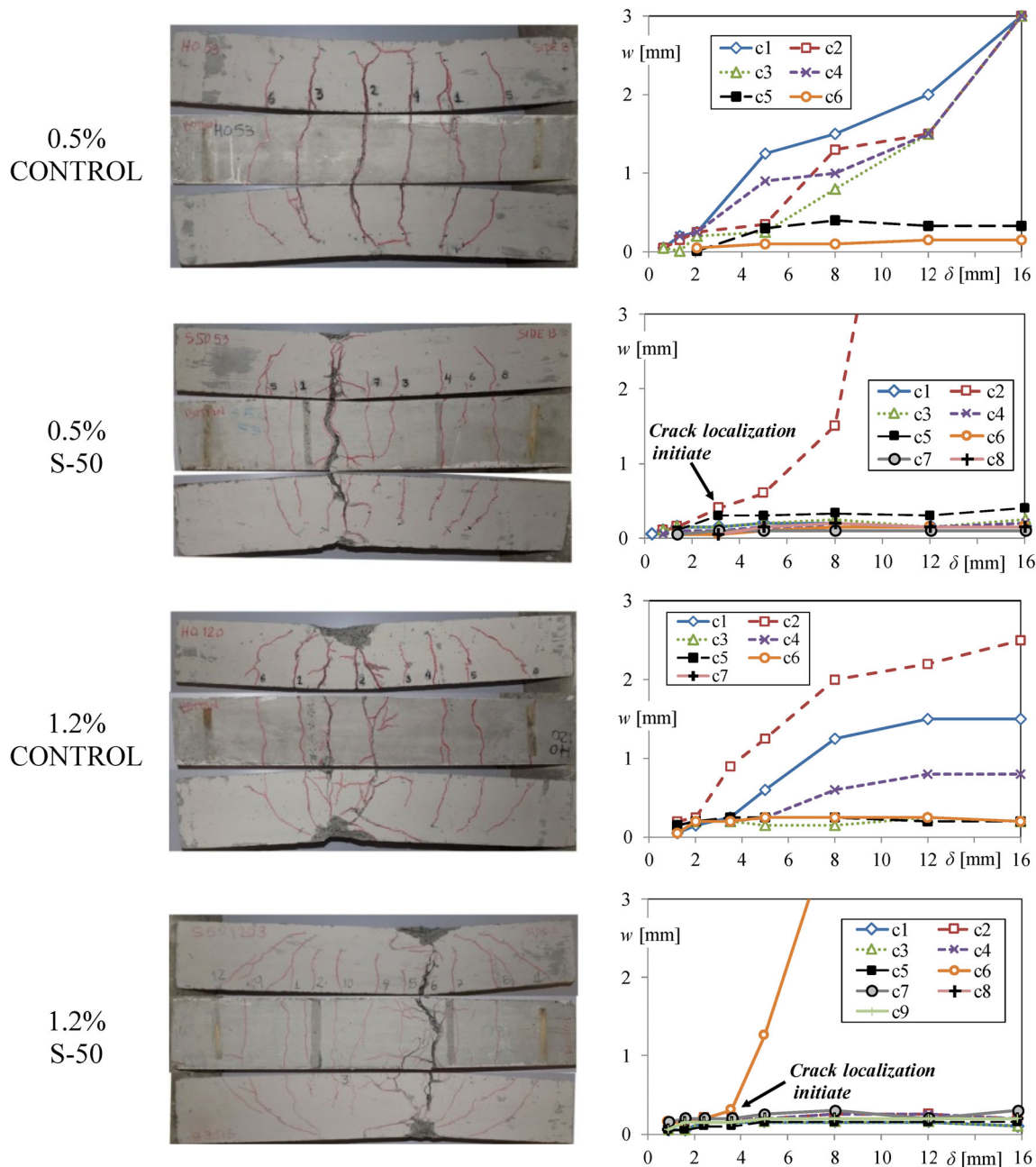
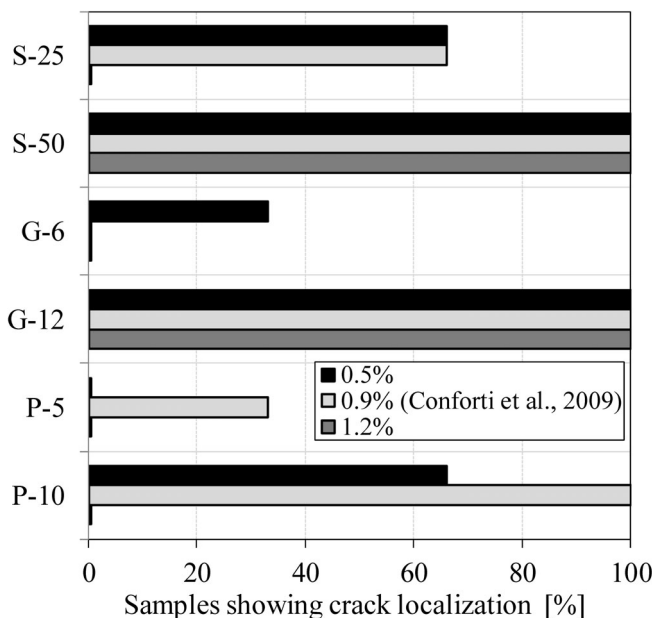


FIGURE 6 Crack development and final crack pattern of CONTROL and S-50 samples with  $\rho_s$  equal to 0.5 and 1.2%

To better understand the different crack development in RC beams with and without fibers, Figure 6 shows the final crack pattern and crack width versus deflection curves of a CONTROL and a S-50 sample for  $\rho_s = 0.5\%$  and  $\rho_s = 1.2\%$ . The main aspects already underlined can be once again observed: clear reduction of crack spacing using steel fibers, especially in the case of  $\rho_s = 0.5\%$ ; reduction of crack spacing passing from  $\rho_s = 0.5\%$  to  $\rho_s = 1.2\%$  (as already acknowledged in the literature,<sup>23</sup>); flexural collapse characterized by compression zone failure after rebar yielding and crack localization when fibers are present. The probability of occurrence of crack localization is summarized in Figure 7 as a function of longitudinal reinforcement ratio for each FRC; a clear relation between crack localization and FRC toughness cannot be established. It can be underlined that crack localization probability increases as FRC toughness increases and as longitudinal reinforcement ratio decreases. The probability of having crack localization is very high using high amount of steel or glass fibers. In addition, this figure shows that the crack localization probability is generally high using fibers, since it is greater than 50% in most of cases. Since the flexural behavior of RC beams at ULS is not related only to the bearing capacity, it is important also to discuss the fiber influence on RC beam ductility, which could be affected by this crack localization. Defining the ductility in terms of displacement as the ratio between  $\delta_u$  and the deflection at rebar yielding ( $\delta_y$ ) and given that  $\delta_y$  is similar for any series, a direct comparison between the values of  $\delta_u$  summarized in both Table 2 and Table 3



**FIGURE 7** Crack localization as a function of longitudinal reinforcement ratio and fiber reinforced concrete series

can be carried out. It results that, even if crack localization took place in several RC beams with fibers (see  $\delta_{CL}$  in Table 2 and Table 3), the ductility of RC beams is not compromised for the typical values of longitudinal reinforcement adopted in practice (in particular for  $0.5\% \leq \rho_s \leq 1.2\%$  and FRC toughness characterized by  $f_{R3}$  varying between 1 MPa and 4.9 MPa). However, crack localization leads to a maximum crack opening after rebar yielding greater in RC beams incorporating fibers than in the case of CONTROL beams, as shown in Figure 6.

## 5 | IMPROVEMENT OF FIB MODEL CODE 2010 FORMULATION

Marching the results of the present experimental campaign with the ones of Conforti et al.,<sup>14</sup> it came out that the formulation of *fib* Model Code 2010 related to mean crack spacing (Equation 1) needs to be improved. In this formulation, the fibers effect is considered as reduction of the introduction length ( $l_{s,max}$ ) by means of the parameter at SLS  $f_{Fts} = 0.45f_{R1}$ . Analyzing Equation (1), it was underlined a progressive reduction of model accuracy increasing  $f_{R1}$  with values of  $s_r/s_{r,MC2010}$  of about 1.4–1.5 for  $f_{R1}$  greater than 3.5 MPa (residual strength range of steel fibers). This experimental evidence is in accordance to the previous results obtained by Tiberti et al.<sup>24</sup> after testing several tension ties, where an important underestimation of mean crack spacing was observed for high values of  $f_{R1}$ . The reasons of this low accuracy can be due to either crack spacing formulation or to adopted *fib* Model Code 2010 linear model for taking into account fiber effect ( $f_{Fts}$ ). In fact, Amin et al.<sup>25</sup> already underlined some criticisms on this linear model, that is, the residual tensile strength of FRC can be overestimated.

In order to figure out if  $f_{Fts}$  is the good parameter representing fiber effects in Equation (1), the axial tensile stress-crack opening ( $\sigma - w$ ) law of the different FRC was obtained by inverse analyses. Numerical analyses on three-point notched prismatic specimens<sup>20</sup> were performed using the FE program DIANA,<sup>26</sup> adopting a discrete crack approach and a tri-linear postcracking law. Figure 8a shows the inverse analyses of the different FRC, obtained by calibrating suitable axial tensile stress-crack opening law. In addition, based on experimental results, it came out that the crack width at stabilized crack stage of the different RC beams is small and in the range between 0.10 and 0.20 mm. Considering an average value equal to 0.15 mm, from the different axial tensile stress-crack opening laws, the mean stress transfer by fibers across cracks can be obtained at stabilized crack stage ( $\sigma_{0.15}$ ). The values of this parameter are summarized in Figure 8a as well. Since  $\sigma_{0.15}$  should

represent the fiber effect at SLS, it was used to substitute  $f_{Fts}$  in Equation (1). This leads to have the following expression:

$$s_{r,FRC} = 1.17 \cdot l_{s,max} = 1.17 \cdot \left[ k \cdot c + \frac{1}{4} \cdot \frac{\emptyset}{\rho_{s,ef}} \cdot \frac{(f_{ct} - \sigma_{0.15})}{\tau_b} \right] \quad (2)$$

The predictions of Equation (2) in comparison with the experimental results are reported in Figure 8b. It can be observed that, using the parameter  $\sigma_{0.15}$  from inverse analyses, the prediction of *fib* Model Code 2010

formulation significantly improves. In particular, the progressive reduction of model accuracy disappeared and the model accuracy is comparable to the case of RC beams without fibers even for high postcracking residual strengths. This evidence underlines that  $f_{Fts}$  is not able to represent the effect of fibers on mean crack spacing. In fact,  $f_{Fts}$  leads to an overestimation of residual strength ( $\sigma_{0.15}$  is always lower than  $f_{Fts}$ ) at stabilized crack stage, which provoke a too high crack spacing reduction as compared to the reality. However, since inverse analysis is not an easy tool for designer, Figure 9a shows the relation between  $\sigma_{0.15}$  and  $f_{Fts}$ . It can be observed that, with

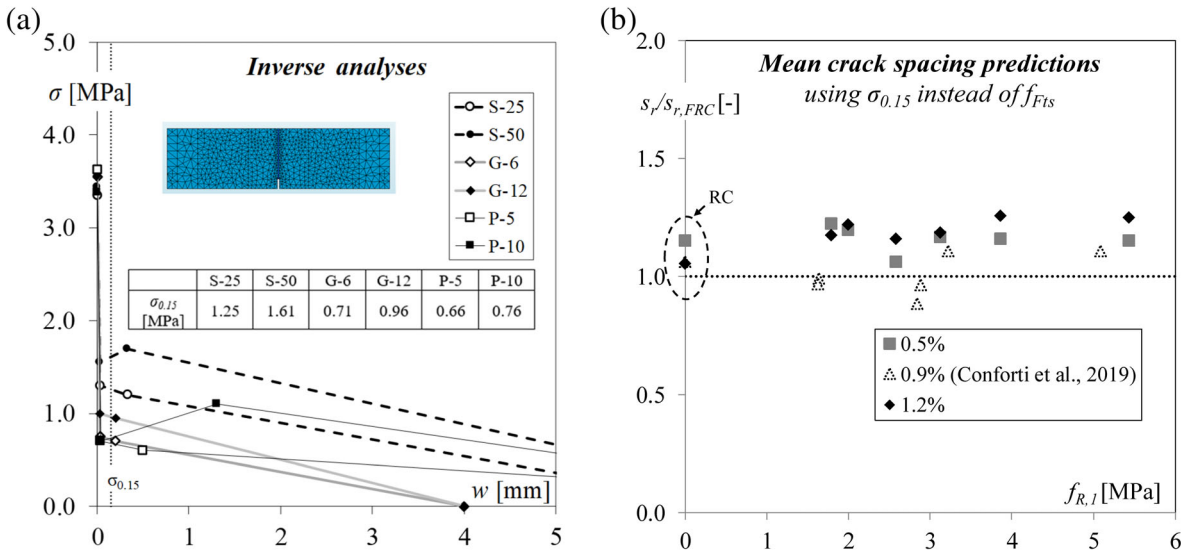


FIGURE 8 Constitutive laws by inverse analyses of the different fiber reinforced concrete (a) and mean crack spacing predictions by using Equation (2) (b)

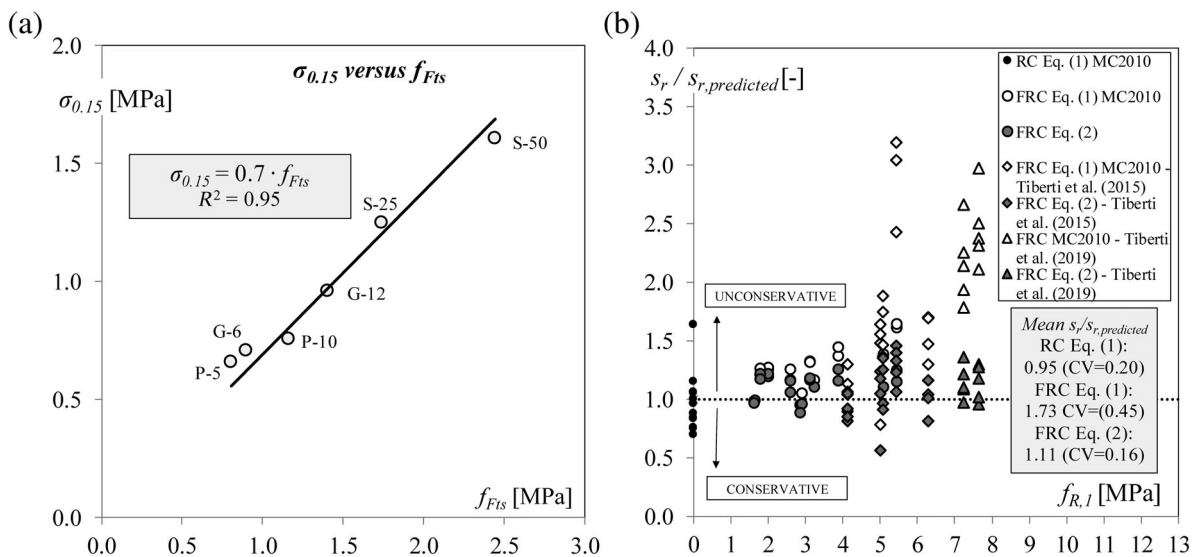


FIGURE 9 Relation between the residual axial tensile strength at a crack opening equal to 0.15 mm ( $\sigma_{0.15}$ ) and the serviceability residual strength  $f_{Fts}$  (a) and crack spacing predictions of *fib* Model Code 2010 (Equation (1)) and Equation (2) considering also results on tension ties present in the literature (b)

good approximation, a linear relation is possible with gradient equal to 0.70. Therefore,  $0.70 f_{Fts}$  could be used instead of  $f_{Fts}$  in *fib* Model Code formulation for mean crack spacing evaluation (considering  $0.70 f_{Fts} < f_{ct}$  or more in general, tension softening behavior under axial tensile forces). Another possibility is to use models present in the literature able to better estimate the value of  $\sigma_{0.15}$  starting from residual strengths of EN 14651,<sup>20</sup> as for example the one proposed by Amin et al..<sup>25</sup> In the latter,  $\sigma_{0.15}$  can be obtained by combining the residual strengths  $f_{R,2}$  and  $f_{R,4}$ .

In order to verify the goodness of Equation (2), since mean crack spacing formulations are generally developed by using experiments on tension ties, predictions of *fib* Model Code 2010 (Equation (1)) and Equation (2) considering  $\sigma_{0.15} = 0.70 f_{Fts}$  were compared against the experimental results obtained by Tiberti et al.,<sup>9,24</sup> where several tension ties in FRC (varying  $c$ ,  $\emptyset$ ,  $\emptyset/\rho_{s,ef}$ ) were tested. Figure 9b shows the ratio between  $s_r$  and the mean crack spacing predicted by either Equation (1) or Equation (2) ( $s_{r,predicted}$ ) as a function of  $f_{R,1}$ . Predictions of RC beams herein tested and RC beams tested by Conforti et al.<sup>14</sup> are reported in circle symbols, while the ones of tension ties from Tiberti et al.<sup>9,24</sup> are indicated in rhombus and triangle symbols. It can be observed that, according also to the results obtained above, *fib* Model Code 2010 formulation becomes more and more unconservative by increasing  $f_{R,1}$ . This leads to an overall ratio  $s_r/s_{r,predicted}$  equal to 1.73 with high CV. Conversely, a significant improvement of predictions is obtained by using Equation (2) and  $0.70 f_{Fts}$ . In fact, predictions are slightly unconservative with a  $s_r/s_{r,predicted}$  ratio closer to the unit (1.11) and the model is not reducing its accuracy by increasing  $f_{R,1}$ . This proves that *fib* Model Code 2010 formulation for mean crack spacing can be easily improved by using a residual tensile strength at  $w = 0.15$  mm (representative of stabilized crack stage), which can be obtained in the first approximation by multiplying  $f_{Fts}$  for a parameter equal to 0.70.

## 6 | CONCLUDING REMARKS

The influence of FRC postcracking performances ( $1.8 \leq f_{R,1} \leq 5.4$  MPa and  $1.0 \leq f_{R,3} \leq 4.9$  MPa) and longitudinal reinforcement ratio ( $0.5\% \leq \rho_s \leq 1.2\%$ ) on the flexural behavior of RC beams was evaluated by means of an experimental program on small-scale beams. Steel, polymer, and glass macrofibers in different amounts were studied. Based on these experimental results, the following conclusions can be drawn:

1. The relations between  $s_r$ ,  $w_{max}$ ,  $\delta$  and  $f_{RI}$  at SLS and between  $P_{max}$  and  $f_{R3}$  at ULS remain mainly linear even varying the longitudinal reinforcement ratio, confirming the independence of these relations from fiber type.
2. The relation between  $s_r$  and  $\emptyset/\rho_{s,ef}$  is still linear adding fibers. However, an increase of  $f_{RI}$  leads to a decrease of line slope. An increase of  $\emptyset/\rho_{s,ef}$  results in a higher crack spacing reduction due to fibers as well.
3. A reduction of maximum crack width is remarkable for values of  $f_{RI}$  greater than 2 MPa (up to 50, 40, and 22% for  $\rho_s$  equal to 0.5, 0.9, and 1.2%, respectively). For  $f_{RI} < 2$  MPa this reduction is lower than 10%.
4. For a longitudinal reinforcement ratio ranging between 0.9 to 1.2%, the deflection reduction at SLS is noteworthy only in the case of  $f_{RI} > 3$ –3.5 MPa (that is the case of steel fibers), while for  $\rho_s = 0.5\%$  even lower values of  $f_{RI}$  are able to lead to a non-negligible deflection reduction. Concerning ULS, the increase of flexural bearing capacity due to fiber is significant only for low longitudinal reinforcement ratios ( $\rho_s$  around 0.5%).
5. Even if the probability of having crack localization increases as FRC residual strength increases and longitudinal reinforcement ratio decreases, a strong relation between crack localization and FRC toughness cannot be established. The probability of crack localization resulted very high in concretes incorporating  $50 \text{ kg/m}^3$  of steel fibers and  $12 \text{ kg/m}^3$  of glass ones.
6. In the typical range of longitudinal reinforcement ratio adopted in practice for RC beams, fibers do not compromise the beam ductility due to crack localization. However, for a given longitudinal reinforcement ratio, a relation between crack localization and FRC toughness cannot be established. It can be only stated that crack localization probability increases as FRC toughness increases and as longitudinal reinforcement ratio decreases.
7. The *fib* Model Code 2010 formulation for bending moment resistance is reliable, while the one regarding mean crack spacing predictions is characterized by a progressive loss of accuracy by increasing  $f_{RI}$  (regardless longitudinal reinforcement ratio). This loss of accuracy is mainly due to parameter chosen by *fib* Model Code 2010 for describing fiber effect, that is,  $f_{Fts}$ . In fact, for a typical value of crack width at stabilized crack stage,  $f_{Fts}$  overestimates the residual tensile stress transfer across cracks by fibers. Based on this experimental program, a residual tensile strength at crack opening equal to 0.15 mm ( $\sigma_{0.15}$ ) was proposed to be used. However, further tests should be carried out in order to prove the reliability of this parameter

by a broad and comprehensive experimental program and if needed, improve it again.

## ACKNOWLEDGMENTS

The authors would like to give their appreciation to Engineers María Celeste Torrijos, Graciela Giaccio, Agustín Rosseti, Juan Carlos Vivas Montes, and Mr. Pablo Bossio for their collaboration in the development of the experimental work.

## LIST OF SYMBOLS

$A_{c,ef}$	effective area of concrete in tension
$A_s$	area of reinforcement
$b_w$	beam web width
$c$	clear concrete cover
CMOD	crack mouth opening displacement
$d$	beam effective depth
$f_c$	mean value of the cylinder compressive concrete strength
$f_{ct}$	mean value of the axial tensile concrete strength
$f_{Fts}$	serviceability residual strength
$f_{Ftu}$	ultimate residual strength
$f_L$	mean value of limit of proportionality
$f_{R,1}$	mean value of residual flexural tensile strength corresponding to CMOD = 0.5 mm
$f_{R,2}$	mean value of residual flexural tensile strength corresponding to CMOD = 1.5 mm
$f_{R,3}$	mean value of residual flexural tensile strength corresponding to CMOD = 2.5 mm
$f_{R,4}$	mean value of residual flexural tensile strength corresponding to CMOD = 3.5 mm
$h$	beam height
$l_{s,max}$	introduction length
$M_u$	flexural strength
$\emptyset$	bar diameter
$P$	load
$P_{cr}$	load at flexural cracking
$P_{max}$	maximum load
$P_{u,MC2010}$	load corresponding to the predicted flexural strength according to <i>fib</i> Model Code 2010
$R^2$	coefficient of determination
$s_r$	mean crack spacing
$s_{r,FRC}$	predicted mean crack spacing considering $\sigma_{0.15}$ in <i>fib</i> Model Code 2010 formulation
$s_{r,MC2010}$	predicted mean crack spacing according to <i>fib</i> Model Code 2010
$s_{r,predicted}$	predicted mean crack spacing
$w$	crack width
$w_m$	mean crack width
$w_{max}$	maximum crack width
$w_{max,P37}$	maximum crack width at $P = 37$ kN
$w_{max,P78}$	maximum crack width at $P = 78$ kN

$\delta$	net mid-span deflection
$\delta_{CL}$	net mid-span deflection at crack localization initiation
$\delta_{CONTROL}$	net mid-span deflection of CONTROL series
$\delta_{P26}$	net mid-span deflection at $P = 26$ kN
$\delta_{P55}$	net mid-span deflection at $P = 55$ kN
$\delta_u$	maximum net mid-span deflection
$\delta_y$	net mid-span deflection at rebar yielding
$\rho_s$	longitudinal reinforcement ratio ( $= A_s/b_w d$ )
$\rho_{s,ef}$	effective reinforcement ratio ( $= A_s/A_{c,ef}$ )
$\sigma$	axial tensile stress
$\sigma_{0.15}$	residual axial tensile strength at $w = 0.15$ mm
$\tau_b$	mean bond stress between steel and concrete

## ORCID

Antonio Conforti  <https://orcid.org/0000-0003-2796-7409>

## REFERENCES

- Amin A, Gilbert RI. Steel fiber-reinforced concrete beams—Part I: Material characterization and in-service behavior. *ACI Struct J*. 2019a;116(2):101–111. <https://doi.org/10.14359/51713288>.
- Amin A, Foster SJ, Kaufmann W. Instantaneous deflection calculation for steel fibre reinforced concrete one way members. *Eng Struct*. 2017;131:438–445. <https://doi.org/10.1016/j.engstruct.2016.10.041>.
- Meda A, Minelli F, Plizzari GA. Flexural behaviour of RC beams in fibre reinforced concrete. *Compos Part B Eng*. 2012; 43(8):2390–2937. <https://doi.org/10.1016/j.compositesb.2012.06.003>.
- Abrishami HH, Mitchell D. Influence of steel fibers on tension stiffening. *ACI Struct J*. 1997;94:769–773.
- Bischoff PH. Tension stiffening and cracking of steel fiber-reinforced concrete. *J Mater Civ Eng*. 2003;15(2):174–182.
- Chiaia B, Fantilli AP, Vallini P. Evaluation of crack width in FRC structures and application to tunnel linings. *Mater Struct*. 2009;42:339–351. <https://doi.org/10.1617/s11527-008-9385-7>.
- Di Carlo F, Spagnuolo S. Cracking behavior of steel fiber-reinforced concrete members subjected to pure tension. *Struct Concr*. 2019;20(6):2069–2080. <https://doi.org/10.1002/suco.201900048>.
- Nguyen W, Bandelt MJ, Trono W, Billington SL, Ostertag CP. Mechanics and failure characteristics of hybrid fiber-reinforced concrete (HyFRC) composites with longitudinal steel reinforcement. *Eng Struct*. 2019;183:243–254. <https://doi.org/10.1016/j.engstruct.2018.12.087>.
- Tiberti G, Minelli F, Plizzari GA. Cracking behavior in reinforced concrete members with steel fibers: A comprehensive experimental study. *Cem Concr Res*. 2015;68:24–34. <https://doi.org/10.1016/j.cemconres.2014.10.011>.
- Amin A, Gilbert RI. Steel fiber-reinforced concrete beams—Part II: Strength, ductility, and design. *ACI Struct J*. 2019b;116(2): 113–123. <https://doi.org/10.14359/51713289>.
- Cuenca E, Conforti A, Minelli F, Plizzari GA, Navarro-Gregori J, Serna P. A material-performance-based database for

- FRC and RC elements under shear loading. *Mater Struct.* 2018; 51(1):11. <https://doi.org/10.1617/s11527-017-1130-7>.
12. Dinh HH, Parra-Montesinos GJ, Wight J. Shear behaviour of steel fibre-reinforced concrete beams without stirrup reinforcement. *ACI Struct J.* 2010;107:597–606.
  13. Ortiz-Navas F, Navarro-Gregori J, Leiva-Herdocia GE, Serna P, Cuenca E. An experimental study on the shear behaviour of reinforced concrete beams with macro-synthetic fibres. *Constr Build Mater.* 2018;169:888–899. <https://doi.org/10.1016/j.conbuildmat.2018.02.023>.
  14. Conforti A, Zerbino R, Plizzari GA. Influence of steel, glass and polymer fibers on the cracking behavior of reinforced concrete beams under flexure. *Struct Concr.* 2019;20(1):133–143. <https://doi.org/10.1002/suco.201800079>.
  15. Schumacher P. Rotation capacity of self-compacting steel fibre reinforced concrete. PhD thesis, TU-Delft; 2006.
  16. Werzbrger S, Karinski YS, Dancygier AN. Quantification of cracking localization in fibre-reinforced concrete beams. *IOP Conf Series: Mater Sci Eng.* 2017;246(1):012024.
  17. Noghabai K. Effect of tension softening on the performance of concrete structures. Experimental, Analytical and Computational Studies. PhD thesis, Div. of Structural Engineering, Lulea University of Technology; 1998; p. 186.
  18. Ghahremannejad M, Mahdavi M, Saleh AE, Abhaee S, Abolmaali A. Experimental investigation and identification of single and multiple cracks in synthetic fiber concrete beams. *Case Studies Constr Mater.* 2018;9:e00182. <https://doi.org/10.1016/j.cscm.2018.e00182>.
  19. Fédération Internationale du Béton. Lausanne, Switzerland: (2012). *fib Model Code 2010 – Final draft [Volume 1, 350 pages, ISBN 978-2-88394-105-2; Volume 2, 370 pages, ISBN 978-2-88394-106-9]*.
  20. EN 14651. Precast concrete products - test method for metallic fibre concrete—Measuring the flexural tensile strength. Brussels, Belgium: CEN; 2005.
  21. EN 15630-1. Steel for the reinforcement and prestressing of concrete—Part 1: Test methods. Brussels, Belgium: CEN; 2004.
  22. Plizzari GA, Serna P. Structural effects of FRC creep. *Mater Struct.* 2018;51:167.
  23. Wight JK, MacGregor JG. Reinforced concrete: Mechanics and design. Prentice Hall, NJ: Pearson, 2009.
  24. Tiberti G, Trabucchi I, AlHamaydeh M, Minelli F, Plizzari GA. Crack development in steel-fibre-reinforced concrete members with conventional rebars. *Mag Concr Res.* 2019;71(11):599–610. <https://doi.org/10.1680/jmacr.17.00361>.
  25. Amin A, Foster SJ, Muttoni A. Derivation of the  $\sigma$ -w relationship for SFRC from prism bending tests. *Struct Concr.* 2015;16(1):93–105. <https://doi.org/10.1002/suco.201400018>.
  26. DIANA – Finite Element Analysis. User's manual release 10.2. Delft, The Netherlands: TNO DIANA BV, 2017. Edited by Jonna Manie and Wijtze Pieter Kikstra.

## AUTHOR BIOGRAPHIES



Antonio Conforti, Ph.D., Assistant Professor, Department of Civil, Environmental, Architectural Engineering and Mathematics (DICATAM), University of Brescia, Italy. [antonio.conforti@unibs.it](mailto:antonio.conforti@unibs.it)



Raúl Zerbino, Associate Professor and CONICET Researcher at LEMIT-CIC, Department of Civil Engineering, La Plata National University, La Plata, Argentina. [zerbino@ing.unlp.edu.ar](mailto:zerbino@ing.unlp.edu.ar)



Giovanni Plizzari, Professor of Structural Engineering, Department of Civil, Environmental, Architectural Engineering and Mathematics (DICATAM), University of Brescia, Italy. [giovanni.plizzari@unibs.it](mailto:giovanni.plizzari@unibs.it)

**How to cite this article:** Conforti A, Zerbino R, Plizzari G. Assessing the influence of fibers on the flexural behavior of reinforced concrete beams with different longitudinal reinforcement ratios. *Structural Concrete.* 2020;1–14. <https://doi.org/10.1002/suco.201900575>